ACS APPLIED POLYMER MATERIALS

pubs.acs.org/acsapm Article

Synthesis and Characterization of Biocompatible Sulfoxide-Containing Molecular Bottlebrushes

Mateusz Olszewski,[⊥] Duy Anh Pham,[⊥] Sara González Bolívar, Jean-Michel Rabanel, Michael Martinez, Krzysztof Matyjaszewski,* and Xavier Banquy*

Cite This: ACS Appl. Polym. Mater. 2022, 4, 8564−8573 Read Online

ACCESS | Metrics & More | Article Recommendations | Supporting Information

ABSTRACT: Macromolecular bottlebrushes (MBs) are emerging as an attractive polymer architecture for biomedical applications. Herein, synthesis and characterization of sulfoxide-containing water-soluble MBs with poly(2-(methylsulfinyl)ethyl acrylate) (PMSEA) side chains with varying grafting densities are reported. Highly hydrophilic PMSEA side chains were prepared by grafting-from poly(2-bromoisobutyryloxyethyl methacrylate) (PBiBEM) using photoATRP with either $CuBr_2$/TPMA (tris(2-pyridylmethyl)amine), $CuBr_2$/TPMA*[3] (tris([(4-methoxy-2,5-dimethyl)-2-pyridyl]methyl)amine), or $CuBr_2$/Me_6TREN (tris(2-dimethylaminoethyl)amine), which were photochemically reduced to the appropriate amount of activators CuBr/ligand to start atom transfer radical polymerization (ATRP). Kinetic experiments showed that the polymerization was the fastest using $CuBr_2$/Me_6TREN at 6-fold excess of ligand to Cu. Additionally, the increase of ligand concentration resulted in a faster reaction with $CuBr_2$/Me_6TREN. A series of PMSEA MBs with grafting densities of 30%, 50%, and 100% was synthesized. The PMSEA MBs exhibited tunable hydrodynamic lubrication properties and low cytotoxicity against different types of cells. PMSEA MBs reveal rheological properties characteristic for nonentangled polymer melts. Densely grafted PMSEA MBs showed a nonlinear relationship between the coefficient of friction and the applied force.

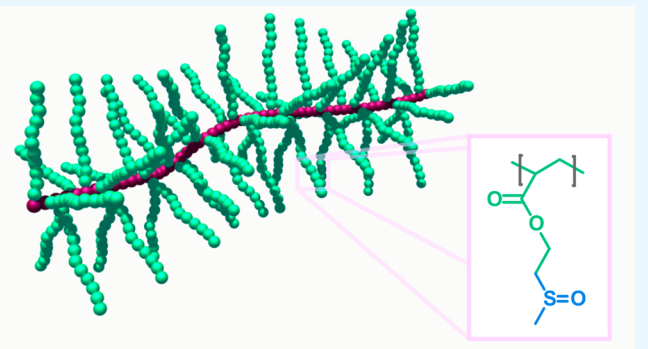

KEYWORDS: *molecular bottlebrushes, controlled radical polymerization, lubrication, thin films, sulfoxides*

INTRODUCTION

Molecular bottlebrushes (MBs) consist of densely grafted side chains along a polymeric backbone. Steric repulsion between the side chains stretches out the backbone, resulting in the MB taking up a rodlike conformation. MBs exhibit a tunable structure, high resistance to compression, and low viscosity in solution due to a lack of entanglement.[1,2] The three main approaches to synthesis of MBs are grafting-from, grafting-through, and grafting-onto. In grafting-from, side chains are polymerized from initiation sites along a premade polymer backbone. Grafting-through is based on polymerization of macromonomers. In grafting-onto, premade side chains are attached to a functionalized backbone via selective coupling techniques, including "click", Diels−Alder chemistry, or disulfide coupling. The effective side chain grafting density depends on the chosen approach. The grafting-through approach ensures a side chain on every repeat unit. However, steric repulsion between large side chains is a significant factor, and preparation of MBs with long side chains is challenging. Due to steric effects, grafting density is usually the lowest using the grafting-onto approach. Grafting-from provides high grafting density, with a high density of functional groups that can be used for additional functionalization.[3]

Because MB length, thickness, and rigidity can be easily tuned, they found use in a wide range of biomedical applications.[4] MBs can serve as effective carriers of therapeutic cargo,[5−7] scaffolds for injectable hydrogels,[8−10] effective lubricants,[11−13] and antifouling agents.[8,14,15] Currently, polyethylene glycol (PEG) and its derivative (meth)acrylates are the polymers of choice in biomedical applications due to their biocompatibility and "stealth" properties.[16] However, the recent rise in anti-PEG antibody results in higher than ever motivation to find alternative polymers.[17] Therefore, development of new types of hydrophilic and biocompatible polymers is needed.

Synthetic hydrophilic polymers recently used in MBs for biomedical research include zwitterionic polymers, polyelectrolytes,[18] polyethylenimine,[19] and poly(dimethylaminoethyl)-methacrylate.[20] We previously reported the preparation of MBs

Received: August 23, 2022
Accepted: October 18, 2022
Published: November 2, 2022

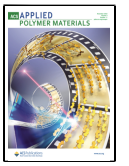

https://doi.org/10.1021/acsapm.2c01468
ACS Appl. Polym. Mater. 2022, 4, 8564−8573

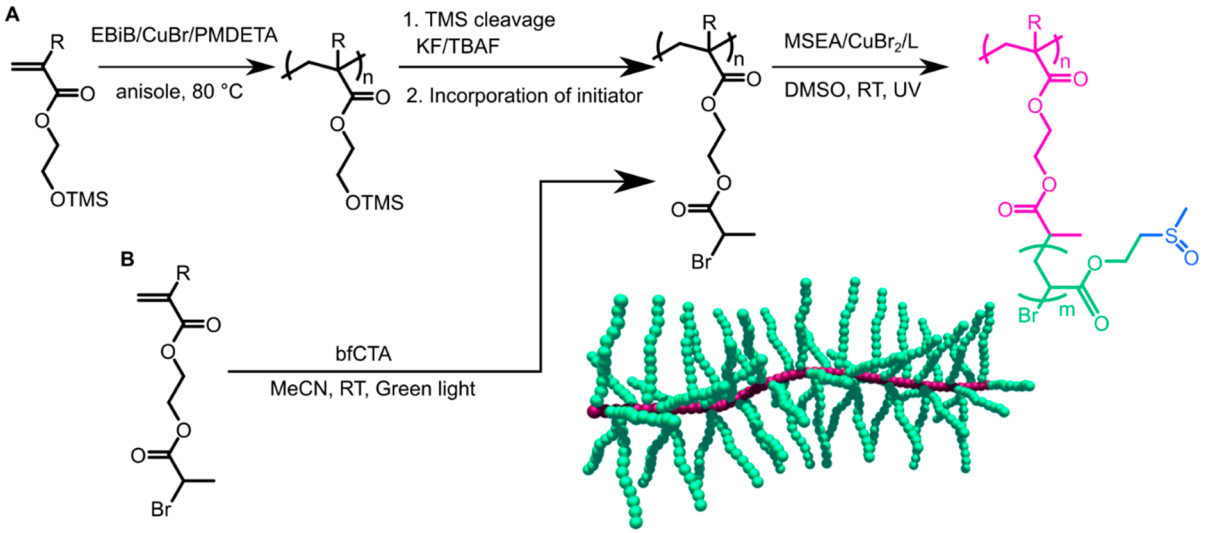

Figure 1. Synthesis of PMSEA MBs by (A) photoATRP from PBiBEM backbone prepared by ATRP and (B) PBiBEM backbone prepared by photoiniferter RAFT.

with poly(2-methacryloyloxyethyl phosphorylcholine) (PMPC) side chains.[21] Monoblock, diblock, and triblock MBs with PMPC brush block and cationic segments had excellent lubrication performance with or without surface modification.[11,22] PMPC MBs showed nontoxic and antifouling behavior.[23,24] There is a growing interest in biocompatible and hydrophilic polymers containing sulfoxide groups, either in the main chain or as pendant groups. Attachment of sulfoxide groups to a polymer aims to overcome the cytotoxicity of small molecules while taking advantage of the unique interactions of sulfoxides with water.[25] Sulfoxide-containing polymers demonstrated potential as antifouling films,[26] agents for nucleotide delivery,[27] and nanogels for skin penetration.[28] Poly(ethyl 2-(methylsulfinyl)acrylate) (PMSEA) is an example of a sulfoxide-containing polyacrylate. It was first synthesized by free radical polymerization,[29] reversible addition−fragmentation chain transfer (RAFT) polymerization,[26] and atom transfer radical polymerization (ATRP).[30−33] PMSEA is highly hydrophilic, exhibits superior low-fouling behavior, and carries low immunogenic risk.[31] Recently, PMSEA with complex architecture was reported, including polymer stars,[31] surface brushes,[26] and bioconjugates.[32]

Herein, we report the first hydrophilic and biocompatible MBs with PMSEA side chains with the aim to evaluate their lubricating and cytotoxic properties. The bottlebrush architecture was chosen due to tunable structure (length, thickness, and rigidity), low compressibility, and low viscosity in solution, which are excellent attributes for lubricating materials. Copolymers with either methyl methacrylate or butyl methacrylate were synthesized to control the density of initiation sites in the polymer backbones and therefore the density of pendant chains. MBs were synthesized via the photoATRP technique from a poly(2-bromoisobutyryloxyethyl methacrylate) (PBiBEM) backbone. Side chains were incorporated using grafting-from of MSEA (Figure 1). Three catalysts were employed: $CuBr_2$/tris(2-pyridylmethyl)amine ($CuBr_2$/TPMA), $CuBr_2$/tris([(4-methoxy-2,5-dimethyl)-2-pyridyl]-methyl)amine ($CuBr_2$/TPMA*[3]), and $CuBr_2$/tris(2-dimethylaminoethyl)amine (Me_6TREN), which were photochemically reduced to the appropriate amount of activators CuBr/ligand to start ATRP. These three catalysts were chosen because of large differences in activity. $CuBr_2$/TPMA*[3] is 1500 times more active than $CuBr_2$/TPMA and 100× more active than $CuBr_2$/Me_6TREN. PMSEA MBs were synthesized with varying densities of grafted side chains. The impacts of grafting density and side chain lengths of PMSEA MBs on their lubrication properties, rheological behavior, and cytotoxicity were also investigated.

MATERIALS AND METHODS

Materials. 2-(Methylthio)ethanol (≥99%) was purchased from Alfa Aesar. Hydrogen peroxide solution (30%) was purchased from Fisher Scientific. Acrylic acid (≥99%), *N*-(3-(dimethylamino)propyl)-*N*′-ethylcarbodiimide hydrochloride (EDC, ≥99%), *N*,*N*-dimethylaminopyridine (DMAP, ≥99%), and copper bromide (≥99.99%) were purchased from Sigma-Aldrich. Acrylic acid was distilled under vacuum before use. Tris(2-dimethylaminoethyl)amine (Me_6TREN, 99%) was purchased from Alfa Aesar and used as received unless otherwise stated. Tris(2-pyridylmethyl)amine (TPMA), tris([(4-methoxy-2,5-dimethyl)-2-pyridyl]methyl)amine (TPMA*[3]), and 2-(methylsulfinyl)ethyl acrylate (MSEA) were synthesized according to previous procedures.[31] A bifunctional CTA, ethane-1,2-diyl bis(4-cyano-4-(((dodecylthio)carbonothioyl)thio)pentanoate) (bfCTA), was synthesized according to a previously reported procedure.[9] 2-(Trimethylsilyloxy)ethyl methacrylate (HEMA-TMS, Aldrich, 96%), *n*-butyl methacrylate (BMA, Aldrich, >99%), and methyl methacrylate (MMA, Aldrich, >99%) were passed through a column filled with basic alumina prior to use to remove any polymerization inhibitor. 2-Hydroxyethyl methacrylate (HEMA, Aldrich, 98%) was purified using the following procedure: First, 2-hydroxyethyl acrylate (HEA) was dissolved in water to form a 33% solution. Then, the solution was washed five times with hexanes. Next, sodium chloride was added to the solution until the formation of a separate layer was observed. The top layer was separated and dried over $MgSO_4$ to obtain pure HEA. All solvents and other chemicals were of reagent quality and were used as received unless special treatments discussed below were applied.

Bottlebrush Polymer Synthesis. *Synthesis of BiBEM.* BiBEM was synthesized using the following procedure (Scheme 1). HEMA (64 mL) was dissolved in dichloromethane (DCM) (1400 mL) and dried over $MgSO_4$. The salts were separated via filtration through a filter paper, and the solution was added directly to a 2 L three-neck round-bottom flask (RBF). Pyridine (47 mL) was added to the RBF. The flask was sealed with two septa and an addition funnel. Nitrogen was bubbled through the solution for 1 h. The flask was lowered into an ice bath before BiBBr (69 mL) was added to the addition funnel

https://doi.org/10.1021/acsapm.2c01468
ACS Appl. Polym. Mater. 2022, 4, 8564−8573

Scheme 1. Synthesis of BiBEM

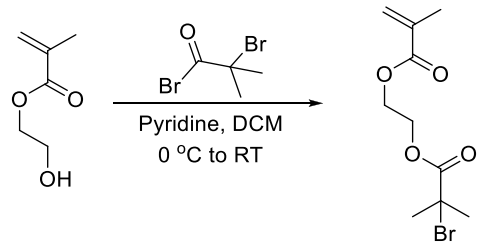

and was added dropwise to the solution overnight. The nitrogen pressure was positive for the duration of the experiment. Most pyridine salts were removed by filtration through filter paper. The crude reaction solution was poured into a 5 L beaker. The mixture was purified by trituration (stirring at 1400 rpm for 10 min in each round) against 2 L solutions of 0.05 M HCl, then 3× saturated sodium bicarbonate, and then 4× deionized water. The aqueous layer was decanted from the solution after each round. The solution was dried over $MgSO_4$ and passed through a basic alumina plug before solvent evaporation on the rotary evaporator. Air was blown over the monomer overnight to remove trace DCM. The concentrated product was passed through a plug of silica before characterization. The monomer was stored inside of a freezer at −20 °C. The yield was 92 g (63%). The purity of the monomer was confirmed by ^{1}H NMR and GC-MS (99.2% purity by abundance)

Step 1a: Synthesis of Poly(HEMA-TMS-co-PMMA) by PhotoATRP. In a typical procedure, a dry 25 mL Schlenk flask was charged with ethyl α-bromoisobutyrate (EBiB, 6 mg, 0.031 mmol), $Cu^{II}Cl_2$ (6 mg, 0.006 mmol), TPMA (10 mg, 0.012 mmol), HEMA-TMS (5.0 g, 5.4 mL, 25 mmol), MMA (2 g, 2.2 mL, 20 mmol), and dimethylformamide (DMF) (1 mL). The solution was degassed by three freeze−pump−thaw cycles. The flask was sealed, evacuated, and backfilled with nitrogen five times and then placed under UV light. The reaction was stopped when the monomer conversion reached 48.9%. The monomer consumption was calculated by the integration of MMA and HEMA-TMS vinyl groups signal (CHH═C−CH_3, 6.11 or 5.56 ppm) against the internal standard (anisole, *o*,*p*-Ar-H, 6.91 ppm). The A block was purified by three precipitations from hexane and then dried under vacuum for 16 h at room temperature.

Step 1b: Synthesis of Poly(HEMA-TMS) by PhotoATRP. In a typical procedure, a dry 25 mL Schlenk flask was charged with ethyl α-bromoisobutyrate (EBiB, 12 mg, 0.062 mmol), $Cu^{II}Cl_2$ (1.22 mg, 0.012 mmol), TPMA (10 mg, 0.025 mmol), HEMA-TMS (5.0 g, 5.4 mL, 25 mmol), and DMF (1 mL). The solution was degassed by three freeze−pump−thaw cycles. The flask was sealed, evacuated, and backfilled with nitrogen five times and then placed under UV light. The reaction was stopped when the monomer conversion reached 27.8%. The monomer consumption was calculated by the integration of MMA and HEMA-TMS vinyl groups signal (CHH═C−CH_3, 6.11 or 5.56 ppm) against the internal standard (anisole, *o*,*p*-Ar-H, 6.91 ppm). Poly(HEMA-TMS) was purified by three precipitations from hexane and dried under vacuum for 16 h at room temperature.

Step 2a: Synthesis of Poly(BiBEM-co-MMA). The polymer from step 1a (2 g, containing 10 mmol of HEMA-TMS units), potassium fluoride (0.689 g, 12 mmol), and 2,6-di-*tert*-butylphenol (204 mg, 1 mmol) were placed in a 50 mL round-bottom flask. The flask was sealed and flushed with nitrogen, and dry tetrahydrofuran (THF) (30 mL) was added. The mixture was cooled in an ice bath to 0 °C, tetrabutylammonium fluoride solution in THF (1 M, 0.105 mL, 0.04 mmol) was injected to the flask, and this was followed by the dropwise addition of 2-bromoisobutyryl bromide (1.47 mL, 12.0 mmol) to form the macroinitiator. After the addition the reaction mixture was allowed to reach room temperature, and stirring was continued for 24 h. The solids were filtered off, and the solution was precipitated into methanol/water (70:30, v/v %). The precipitated macroinitiator was redissolved in chloroform and passed through a short column filled with basic alumina. The filtrate was reprecipitated three times from chloroform into hexanes and dried under vacuum overnight at room temperature.

Step 2b: Synthesis of Poly(BiBEM-co-BMA) by RAFT. BiBEM (1.8 mL, 8.4 mmol), bifunctional CTA, ethane-1,2-diyl bis(4- 123 cyano-4-(((dodecylthio)carbonothioyl)thio)pentanoate) (bfCTA) (0.31 mL of a 0.226 g/mL stock solution in DMF, 84 μmol), BMA (2.68 mL, 16.8 mmol), MeCN (4.5 mL), and a magnetic stir bar were added to a 25 mL Schlenk flask. The flask was wrapped with aluminum foil and sealed with a glass stopper. It was sparged with nitrogen for 30 min. The first aliquot was removed for ^{1}H NMR analysis after degassing the syringe headspace. The reaction was lowered into the photoreactor and was started by turning on the green light. Aliquots were taken to determine the monomer conversion by ^{1}H NMR using the $-CH_2-$ methylene protons for the monomer and polymer within a range of 3.8−4.6 ppm at the internal standard. The conversion of BiBEM and BMA were tracked by their respective vinyl protons. BiBEM conversion was taken as the disappearance of vinyl peak A (6.14 ppm, singlet), and BMA conversion was taken as the disappearance of vinyl peak C (6.09 ppm, singlet). The number-average molecular weight ($M_{n,GPC}$) and dispersity ($Đ$) of each kinetic point were determined by THF GPC relative to linear PMMA standards. BiBEM reached 96% conversion, and BMA reached 98% conversion. GPC analysis of the crude backbone gave $M_{n,GPC}$ = 36 350 and $Đ$ = 1.32. The polymer macroinitiator was purified by precipitation into hexane once before it was dialyzed against acetone. The polymer was isolated as a film under vacuum. The final composition was confirmed by ^{1}H NMR.

Step 2c: Synthesis of polyBiBEM. The polymer from step 1b (0.84 g, containing 4.15 mmol of HEMA-TMS units), potassium fluoride (0.289 g, 4.98 mmol), and 2,6-di-*tert*-butylphenol (86 mg, 0.690 mmol) were placed in a 50 mL round-bottom flask. The flask was sealed and flushed with nitrogen, and dry THF (30 mL) was added. The mixture was cooled in an ice bath to 0 °C, tetrabutylammonium fluoride solution in THF (1 M, 0.042 mL, 0.04 mmol) was injected to the flask, and this was followed by the dropwise addition of 2-bromoisobutyryl bromide (0.616 mL, 5.0 mmol) to form the macroinitiator. After the addition the reaction mixture was allowed to reach room temperature, and stirring was continued for 24 h. The solids were filtered off, and the solution was precipitated into methanol/water (70:30, v/v %). The precipitated macroinitiator was redissolved in chloroform and passed through a short column filled with basic alumina. The filtrate was reprecipitated three times from chloroform into hexanes and dried under vacuum overnight at room temperature.

Step 3: Synthesis of PMSEA Bottlebrush by Grafting-from via PhotoATRP in DMSO. In a typical procedure, a dry 5 mL Schlenk flask was charged with macroinitiator (from step 2a or 2c) (4.3 mg, 0.04 μmol of PBiBEM), MSEA (500 mg, 3.1 mmol), TPMA (0.8 mg, 0.003 mmol), $Cu^{II}Br_2$ (as a stock solution, 0.1 mg, 0.0005 mmol), DMF (0.3 mL), and dimethylsulfoxide DMSO (2.0 mL). The solution was degassed by three freeze−pump−thaw cycles. The flask was sealed, evacuated, and backfilled with nitrogen five times and then placed under UV light. The first kinetic aliquot was taken using an air-free syringe after starting the reaction upon exposure to UV light. After various reaction times, kinetic samples were taken and quenched by exposure to air. The bottlebrush polymer was purified by dialysis against MeOH for 48 h using tubes with a pore size molar mass cutoff of 10 000 kDa.

Step 4: Synthesis of PMSEA Bottlebrush by Grafting-from via PhotoATRP in Acetonitrile. In a typical procedure, a dry 5 mL Schlenk flask was charged with macroinitiator (from step 2b) (9.0 mg, 0.05 μmol of 2b), MSEA (500 mg, 3.1 mmol), TPMA*[3] (0.4 mg, 0.001 mmol), $Cu^{II}Br_2$ (as a stock solution, 0.2 mg, 0.002 mmol), DMF (0.3 mL), and acetonitrile (2.0 mL). The solution was degassed by three freeze−pump−thaw cycles. The flask was sealed, evacuated, and backfilled with nitrogen five times and then placed under UV light. The first kinetic aliquot was taken using an air-free syringe after starting the reaction upon exposure to UV light. After various reaction times, kinetic samples were taken and quenched by exposure to air.

https://doi.org/10.1021/acsapm.2c01468
ACS Appl. Polym. Mater. 2022, 4, 8564−8573

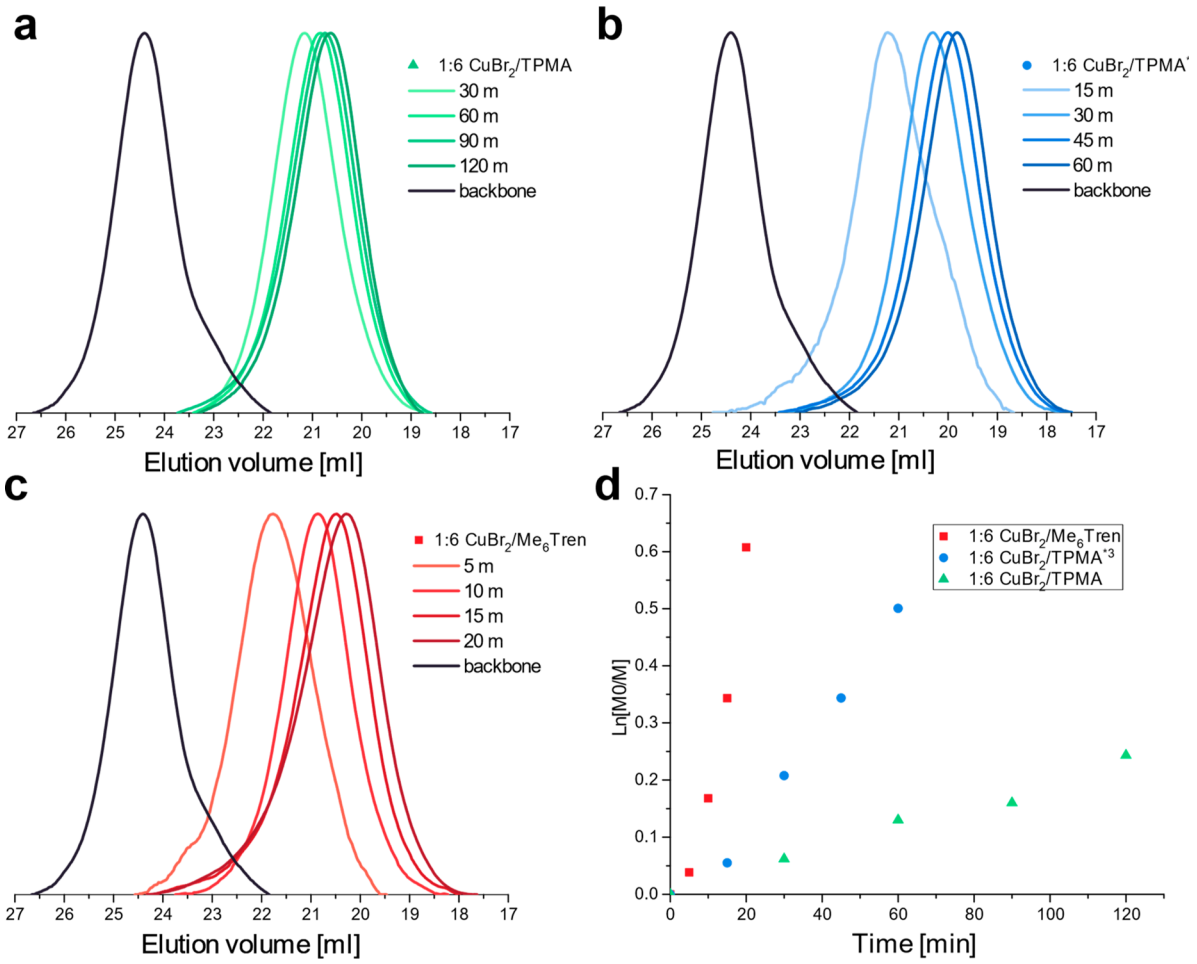

Figure 2. Author: GPC traces of elution during the synthesis of P(BiBEM-*g*-PMSEA) with (a) 1:6 ratio of $CuBr_2$/TPMA, (b) 1:2 ratio of $CuBr_2$/TPMA*[3], and (c) 1:2 ratio $CuBr_2$/Me_6Tren. (d) Pseudo-first-order kinetic plots for the polymerization of poly(n-butyl acrylate) (PBA) molecular bottlebrushes. Irradiation by 360 nm at 4.9 mW/cm^2 at room temperature 25 °C, 75 vol % DMSO, 5% DMF. [MSEA]/[EBiB]/[CuBr2]/[L] = 200:1:0.03:0.18, x = 0.03.

The bottlebrush polymer was purified by dialysis against MeOH for 48 h using tubes with a pore size molar mass cutoff of 10 000 kDa.

Equipment and Analysis. Proton nuclear magnetic resonance (^{1}H NMR) spectroscopy was performed using a Bruker 300 MHz spectrometer. In all cases deuterated chloroform ($CDCl_3$) was used as a solvent, except for the bottlebrush polymer, which was analyzed using deuterated DMSO (DMSO-d_6). ^{1}H chemical shifts are reported in parts per million (ppm) downfield from tetramethylsilane (TMS). Apparent molecular weights and molecular weight distribution measurements of polymers except for the bottlebrush polymer were measured by size exclusion chromatography (SEC) using Polymer Standards Services (PSS) columns (guard, 10^5, 10^3, and 500 Å), with THF or DMF as the eluent at 35 °C at a constant flow rate of 1.00 mL/min, and a differential refractive index (RI) detector (Waters). The apparent number-average molecular weights (M_n) and molecular weight distributions (M_w/M_n) were determined with a calibration based on linear poly(methyl methacrylate) (PMMA) standards and toluene as an internal standard.

Cell Cytotoxicity Experiments. *Polymer Stock Solution and Dilution Preparation.* Each MB polymer (250 μL) in methanol stocked at −80 °C (concentrations: 2−4 mg/mL) were sterile-transferred to autoclaved Eppendorf tubes. After drying, polymers 1 and 2 were resuspended in 250 μL of sterile DPBS, and polymers 3 and 4 were resuspended in 500 μL of sterile DPBS to a final concentration of 10 mg/mL. A serial dilution in sterile DPBS was performed to obtain solutions with final concentrations at 1000, 100, 10, 1, and 0.1 μg/mL (tests with HeLa, MCF-7, and U87 cells); 1000, 500, 100, 10, and 1 μg/mL (tests with Hep G2 and THP-1 cells).

Cell Culture. Dulbecco's modified Eagle's medium (DMEM), RPMI 1640 medium, fetal bovine serum (FBS), penicillin−streptomycin 100× solution, and Dulbecco's phosphate-buffered saline (DPBS) were provided by Wisent, Inc. (Saint-Bruno, QC, Canada). The MTS assay kit was from Abcam, Inc. (Toronto, ON, Canada). HeLa (human cervical cancer cells), U87 (human primary glioblastoma cell line), MCF7 cells (human breast cancer cell line), and Hep G2 (human hepatocyte cell line) were used for cytotoxicity evaluation and cultured in DMEM supplemented with 10% FBS and 1% streptomycin/penicillin. THP-1 (human monocyte cell line) was also used for cytotoxicity assays and cultured in RPMI 1640 medium, supplemented with 10% FBS, 1% streptomycin/penicillin, and 2-mercaptoethanol to a final concentration of 0.05 mM. The cells were maintained in T-75 flasks at 37 °C and 5% CO_2. After trypsinization, the cells were counted and resuspended in complete medium. Seeding density in 96-well plates was determined for each cell line to optimize the assays—HeLa, MCF-7, and Hep G2: 10 × 10^3 cells per well; U87: 5 × 10^3 cells per well; and THP-1: 15 × 10^3 cells per well.

Cells were incubated for 24 h to allow attachment or/and growth. Following attachment, the medium was changed and 10 μL of MB polymer dilution was added (n = 5/concentration), except for THP-1 (nonadherent cell line), for which the medium was not changed. One positive (treatment with DPBS alone) and negative (no cells) control were included in each plate (n = 5). Cells were incubated for 24 h in a cell culture incubator at 37 °C and 5% CO_2.

MTS Cell Proliferation Assay. Cell proliferation after polymer exposure was measured using the MTS Cell Proliferation Colorimetric assay kit (Abcam, Inc., product no. ab197010), used as

https://doi.org/10.1021/acsapm.2c01468
ACS Appl. Polym. Mater. 2022, 4, 8564−8573

recommended by the manufacturer. The absorbance was measured at 470 nm using a Tecan Spark microplate reader (Tecan, Austria). The absorbance was proportional to cell proliferation, and the results were expressed as the average percentage of cell proliferation ± SD.

Surface Forces Experiments. The surface forces apparatus 2000 (SFA 2000, SurForce, LLC, U.S.A.) was used to measure the interaction forces and the distance between two opposing and atomically flat mica surfaces covered with MB polymer. The distance between the surfaces was assessed using the fringes of equal chromatic order (FECO) via multiple beam interferometry (MBI).[34] Displacement of the surfaces was controlled by a coarse differential micrometer manipulated by hand and by a micromotor for the fine (subnanometer) displacement.[35]

Surface Preparation. Back-silvered mica surfaces were prepared by cutting freshly cleaved mica sheets with a thickness of 1−3 μm using a hot platinum wire and then coating one face with silver by physical vapor deposition (Covap, Angstrom Engineering, Canada). Two back-silvered mica pieces having the same thickness were glued (silver side down) on cylindrical glass discs with a curvature of 2 cm. The glass discs carrying the mica sheets were mounted in a cross-cylindrical geometry in the chamber of an SFA and brought into contact in dry air to set the reference contact point. FECO were generated by multiple reflection of a white light beam between the two back-silvered mica sheets and were recorded using a spectrometer and a charge-coupled device (CCD) camera (Andor Technology, U.S.A.). After this calibration, the bottlebrush polymer solution was inserted in between the mica surfaces at a concentration of 100 $\mu g/mL^{-1}$ and left to adsorb for 45 min. Water was also added at the bottom of the SFA chamber to saturate the chamber and limit the evaporation of the liquid between mica surfaces.

Friction Force Measurements. For the assessment of friction force, each MB polymer was tested in at least 3 independent experiments at 2 different contacts in each experiment to ensure reproducibility. The friction force was measured at different normal loads ranging from 0.1 to 5 mN. Back and forth shear cycles were applied when the surfaces were in close contact. For each experiment, 4−10 shearing cycles were applied at each increasing load to ensure that the lubrication properties of the MB layer were stable. The surfaces were sheared past each other using a piezoelectric bimorph designed with a flexure point in the middle, which caused the surfaces to displace linearly as the voltage was applied. The bimorph drove the lower surface in a back-and-forth motion using a triangular wave function with a typical frequency of 50 mHz and an amplitude of 5 V (equivalent to 3 $\mu m/s^{-1}$) controlled by a function generator (Agilent 33250A, Agilent Technologies, Inc., U.S.A.). During sliding, the friction transmitted to the upper surface was measured by two vertical double-cantilever springs equipped with four semiconductor strain gauges attached symmetrically to oppositely bending arms of the springs, thus forming the four arms of a Wheatstone bridge strain gauge system.[35] When a lateral force was applied to the upper surface, the strain gauges were used to measure the deflection with a signal conditioning amplifier (Vishay Measurements, 2310B), which outputs the signal to a computer data-acquisition system.

RESULTS

Synthesis of PMSEA MBs. Grafting-from ATRP of MSEA from a poly(2-bromoisobutyryloxyethyl methacrylate) (PBiBEM) polymer with a degree of polymerization (DP) equal to 372 was used to find the optimal catalyst system. The efficiencies of ATRP catalysts with three different ligands—TPMA, TPMA*[3], and Me_6Tren—were compared. The reactions were stopped upon observing a significant increase in solution viscosity, at ∼40% monomer conversion for all samples. Initially, experiments with 2-fold excess of ligand to $CuBr_2$ were performed. The catalyst with TPMA as a ligand required the longest time to reach a significant monomer conversion, 2 h (see Figure S1) for ∼25% monomer conversion.. Polymerization was significantly faster with both TPMA*[3] and Me_6Tren. Well-defined MBs with low dispersity were obtained for all three systems. No significant differences in dispersity or molecular weight of final brushes were observed despite different reaction times (Table S1).

Next, a series of experiments were performed using a 6-fold excess of ligand to $CuBr_2$. The reaction with Me_6Tren was significantly faster than those with TPMA or TPMA*[3]. A clear trend was observed with TPMA*[3] being slower than Me_6Tren and unmodified TPMA being the slowest (Figure 2).

In ATRP, an increase of polymerization rate with increasing excess of ligand to Cu is typically observed because the ligand acts as an electron donor helping the reduction of the Cu(II) deactivator to the Cu(I) activator complex.[36,37] An excess of Me_6Tren with four tertiary alkyl amine groups, which are more efficient electron donors than aromatic pyridines, accelerated polymerization.

Then, a series of PMSEA MBs with different grafting densities and backbone lengths was synthesized. First, a series of backbones was prepared, with predetermined densities of ATRP initiation sites of approximately 30%, 50%, and 100%. Backbones with different densities of initiation sites were prepared by adjusting the content of MMA or BMA. A backbone with 100% grafting density was prepared by homopolymerization of HEMA-TMS. Backbones with a lower density of initiators were prepared by copolymerization of HEMA-TMS or BiBEM with either MMA or BMA, resulting in polymers where ∼30% or ∼50% of the repeat units contain the ATRP initiator functionality. Side chains were synthesized using grafting-from ATRP of MSEA. TPMA*[3] was used as the ligand to provide a short reaction time and greater control over the final side chain DP. Table 1 contains detailed information about the structures of the prepared samples (GPC traces are provided in Figures S3−S6, and ^{1}H NMR spectra of samples MB1 and MB3 are provided as examples in Figures S7 and S8).

Table 1. Summary of Characterized PMSEA-MB Samples (See Figure S2 for Schematic of the Structures)

entry	backbone DP	grafting density	side chain DP	$M_{n,th} \times 10^{-3}$	$Đ$
MB1	221	∼50%	55	940	1.29
MB2	487	∼50%	54	2290	1.19
MB3	292	∼30%	64	1040	1.25
MB4	372	∼100%	55	3907	1.20

Cellular Toxicities of the Different PMSEA MBs. To evaluate the toxicities of the PMSEA MBs, we chose three epithelial cell lines coming from different organs—cervix, brain, and breast epithelium—and in addition two more cell lines, one from the liver (hepatocytes) and another one from the mononuclear phagocyte system (macrophages). These cell lines are representative of tissues most likely exposed to nanomaterials entering the bloodstream. The polymers dissolved in DPBS did not significantly affect the proliferation of immortalized cancer cells, as shown in Figure 3. From the proliferation assay, no lethal concentration (LC50) could be extracted in the range of polymer concentration tested; therefore, PMSEA MBs appeared to be well-tolerated even at the maximum concentration tested (1 mg/mL). More variability was observed with the MCF7 cell line, but no trend or explanation could be identified. No changes of cell morphology upon MB polymer exposure were detected,

https://doi.org/10.1021/acsapm.2c01468
ACS Appl. Polym. Mater. 2022, 4, 8564−8573

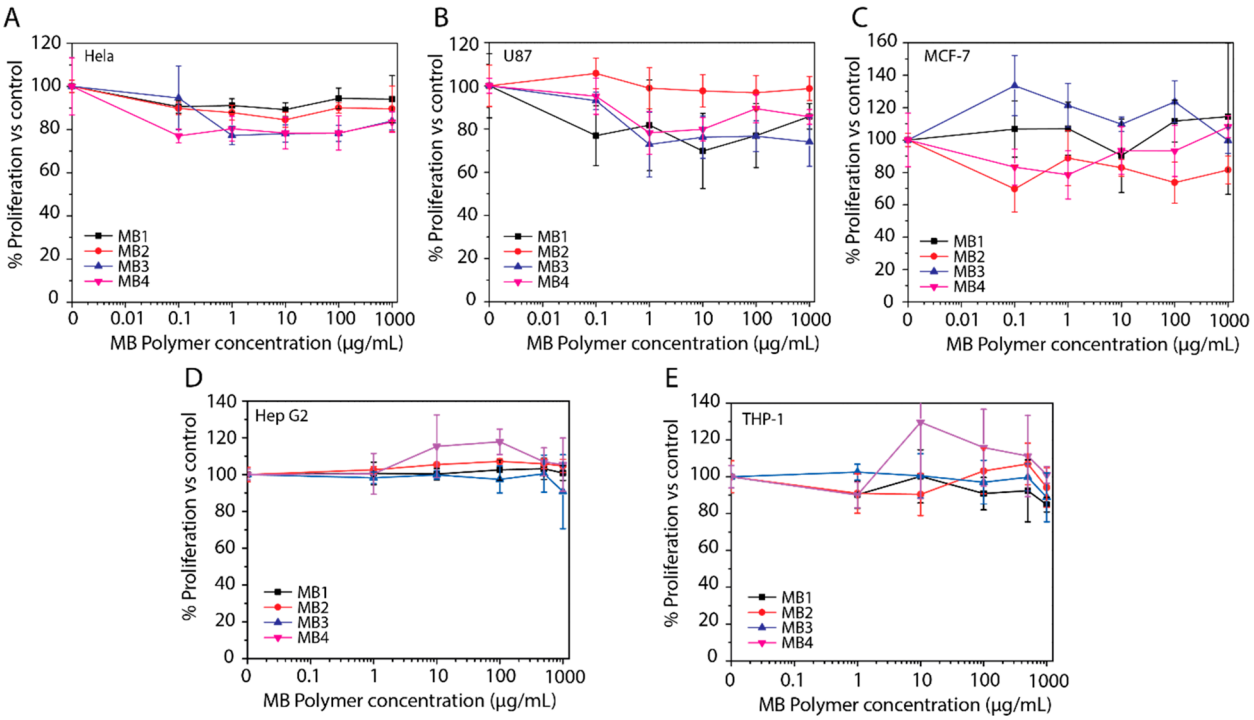

Figure 3. PMSEA MBs do not impact cell proliferation in several cell lines. (A) HeLa, human cervical cancer cell line; (B) U87, human primary glioblastoma cell line; (C) MCF-7, human breast cancer cell line; (D) Hep G2, hepatocyte cell line; (E) THP-1 human monocyte cell line. Cells were exposed for 24 h to different concentrations of PMSEA MBs (n = 5) prior to cell-proliferation assays. Results are expressed as a percentage of proliferation relative to DPBS-treated cells (control).

suggesting that the MB surface groups did not affect the cell membrane integrity (see Figure S9). These results suggest the suitability of PMSEA MBs for therapeutic intervention such as drug delivery, imaging, and lubrication, among others.

Lubrication Properties of the Bottlebrush Polymers. In a first series of tests, the different PMSEA MBs were independently evaluated for their tribological properties against mica surfaces. The mica surface is a good model surface because it is atomically flat and transparent, which facilitates the acquisition of the FECO fringes, and it is brittle and prone to wear. As shown in Figure 4A, the tested polymers exhibited different tribological behaviors depending on their architecture. The measured friction force showed a nonlinear dependence with the applied normal load for all the polymers, a behavior that will be explained in detail later. An effective friction coefficient, μ_{eff}, was estimated using the relationship $\mu_{eff} = dF_s/dF_n$.

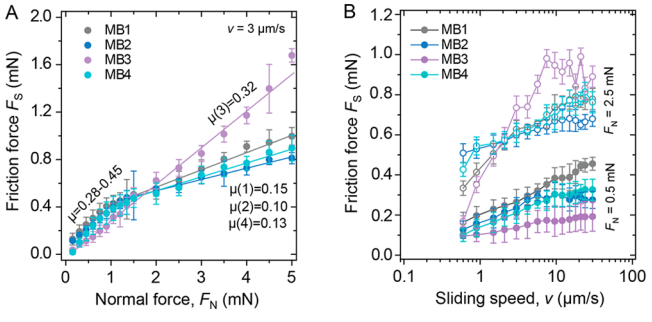

Figure 4. (A) Tribological testing of the 4 different PMSEA MBs in water at 100 μg/mL. Evolution of the friction force with the normal force applied at a constant sliding speed of 3 $\mu m/s^{-1}$. (B) Friction force vs sliding speed at normal loads of 0.5 mN (filled symbols) and 2.5 mN (open symbols).

Author: As can be seen in Figure 4A, at a normal force F_N < 1 mN, a high friction coefficient was measured with μ_{eff} varying between 0.28 and 0.45 depending on the polymer, and for F_N > 1 mN, μ_{eff} was found to vary between 0.104 and 0.154. The coefficient of friction, μ_{eff}, of this load regime was reduced by ~55−70% compared to the low F_N regime. The nonlinear relationship between F_S and F_N was not clearly observed for MB3; therefore, its coefficient of friction remained constant in the whole range of normal force tested but still similar to the values obtained for the other polymers in the low-load regime (μ_{eff} = 0.32). The nonlinearity between F_S and F_N observed for MBs 1, 2, and 4 can be explained by assuming that the shear stress is independent of the load and that there is a Hertzian contact between the two surfaces. In that approximation, F_S and F_N are proportional as

$$F_S \propto F_N^{2/3} \quad (1)$$

and the friction coefficient μ, defined as $\mu = F_S/F_N$, varies as $\mu \propto F_N^{-1/3}$.[38]

As can be seen in Figure 5A, fitting the experimental result with eq 1 was not possible for MB3 but was possible for the other polymers (only the fitting for MB4 is shown for clarity). When monitoring the film thickness during sliding at constant speed, v = 3 μm/s, it appears that the MB3 lubricating film reaches values close to 2 nm at the highest applied load (F_N = 5 mN), which corresponds to the thickness of a monolayer of MB polymer (Figure 5B). The lubricating film at such a high load was the thinnest for MB3 and increased in the order MB3 > MB1 > MB4 > MB2. The increase of the film thickness from MB3 to MB1 and to MB4 is correlated to the increase of the side chain grafting density from 30% to 100% in these

https://doi.org/10.1021/acsapm.2c01468
ACS Appl. Polym. Mater. 2022, 4, 8564−8573

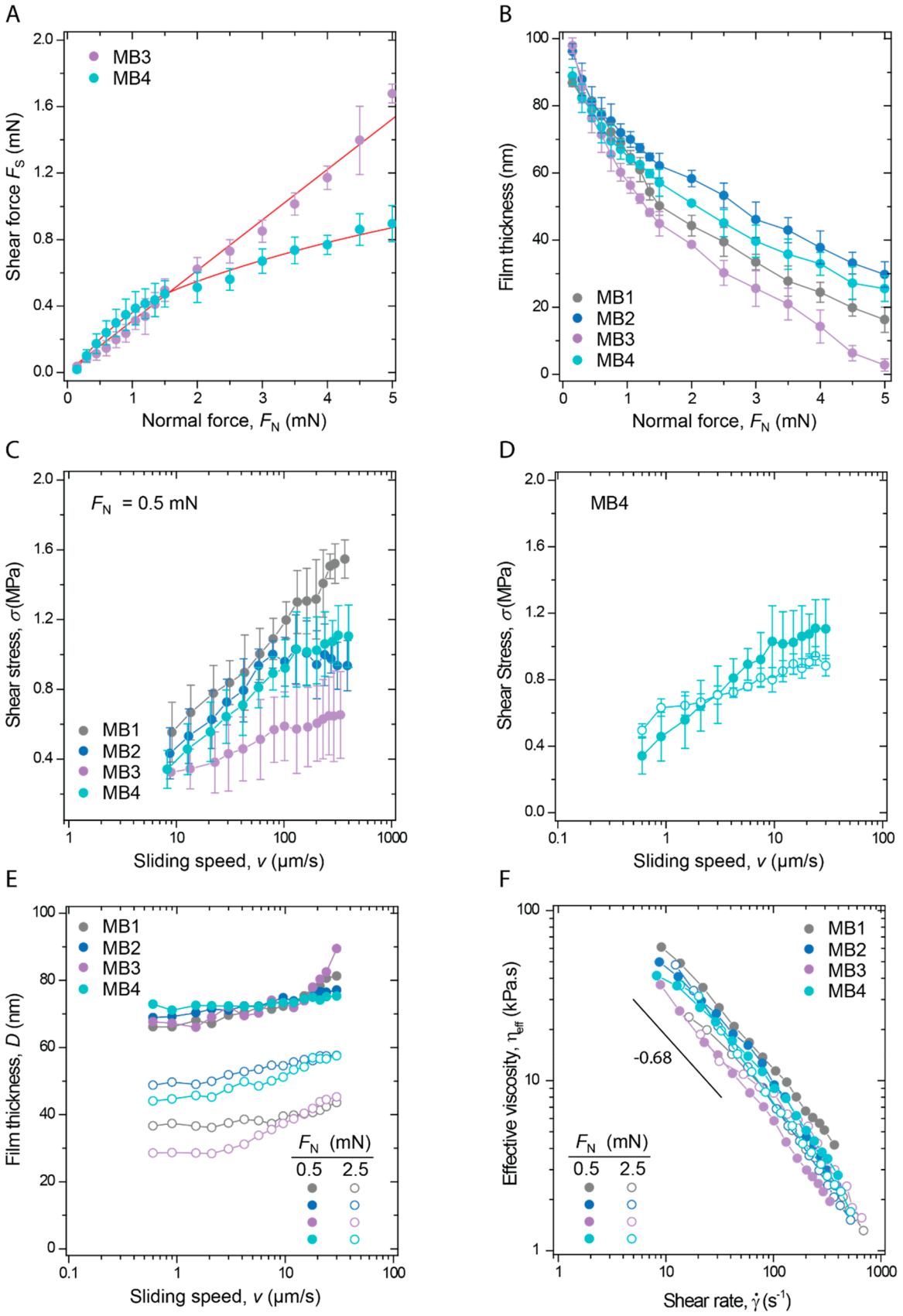

Figure 5. (A) Representative evolution of the shear force as a function of the applied normal force for two bottlebrush polymers behaving significantly differently. (B) Thinning of the polymer film during the shear test. (C) Evolution of the shear stress with the sliding speed for all 4 polymers at low applied normal force and (D) comparison of the shear stress at two different loads. (E) Increase of the lubricating film thickness with the sliding speed at two different applied normal forces and (F) evolution of the effective viscosity with the shear rate at the same two applied normal forces.

https://doi.org/10.1021/acsapm.2c01468
ACS Appl. Polym. Mater. 2022, 4, 8564−8573

polymers. The film thickness of MB2, which has a chain grafting density of 50%, identical to that for MB1, was the largest, probably due to the fact that the backbone length of this polymer was the longest of the series of PMSEA MBs. The values of the hard wall thickness (measured at the highest compression) provide some indications of the conformation of the polymers under confinement. The increase of the hard wall thickness with the length of the backbone of the polymer suggests that its conformation is not flat on the surface, even under high compression, but rather coiled or possibly entangled with other chains.

The large values of the lubricating film thickness at $F_N < 0.5$ mN for all of the polymers also suggest that the lubrication mechanism should be dominated by hydrodynamic lubrication. This could be corroborated by two independent observations. First, in Figures 4B and 5C, the dependence of F_S or the shear stress σ with the sliding speed shows a logarithmic increase, which has been reported for several polymeric lubricating materials exhibiting complex rheological behavior.[39,40] Second, for all four PMSEA MBs, the shear stress extrapolates to zero at zero speed, as shown in Figure 5C, and the shear stress was weakly dependent on the normal force F_N (Figure 5D). Third, we observed a slight increase of the film thickness with the sliding speed at high and low applied loads (thin and thick lubricating films, Figure 5E), which is also a strong indicator of hydrodynamic lubrication. These observations point to a hydrodynamic dissipation mechanism of the friction force, as already reported for polymeric melts.[41]

For a confined fluid, where hydrodynamic dissipation is expected to dominate, an effective thin film viscosity, η_{eff}, can be defined as $\eta_{eff} = F_S D/Av$, where A is the contact area and D is the film thickness. For separation distances that are several times larger than the characteristic size of the molecules constituting the lubricating film, η_{eff} is expected to equal the bulk viscosity. In the present case, this situation is expected to happen when D is superior to a few hundred nanometers based on the size of the backbone of the polymers, which is larger than the separation distance measured during the tribological tests. In Figure 5F is shown the dependence of η_{eff} with the shear rate, $\dot{\gamma}$, for the four different polymers. The effective viscosity is clearly decreasing as $\dot{\gamma}$ increases and follows a power law $\eta_{eff} \propto \dot{\gamma}^n$, with n having the experimental value of $n = -0.68 \pm 0.05$ for all of the polymers. This experimental value is close to the theoretical value of $-2/3$ expected for nonentangled polymer melts[42] and is significantly lower than the value of $n = 1$ reported for polybutadiene melts with molecular weights higher than the molecular entanglement weight, M_e.[43] A similar value for n was obtained for physisorbed polyethylene glycol brushes on mica surfaces in water.[44] Compared to linear polymers, bottlebrush polymers have the singular property to exhibit low entanglement density or high M_e. The scaling of M_e with the molecular diameter of the bottlebrush chain, Δ, is found to scale as $M_e \approx \Delta^3$.[45] Therefore, it is not surprising that the rheological behavior of the MB polymers is close to what is expected for nonentangled polymer melts even when the film thickness D is far larger than Δ. Experimental data show that there are no significant differences in thin film viscosity, η_{eff}, among the 4 polymers, which is likely due to the fact that all of their side chains have the same DP_n and, therefore, the same value of Δ. Data in Figure 5F also show that differences in η_{eff} values between the different polymers are more pronounced at low applied load (large separation distances) than at high applied load (small separation distances). Because the 4 polymers have a backbone DP_n ranging from 219 up to 497, this observation suggests that the thin film viscosity of bottlebrush polymers under high confinement does not depend on the polymer backbone length.

CONCLUSIONS

In this study, a series of molecular bottlebrushes with sulfoxide-containing side chains was synthesized. Kinetic experiments on photoATRP of MSEA from polyacrylate backbones showed significantly faster polymerization with Me_6Tren compared to TPMA or TPMA*[3] when a high excess of ligand was used. PMSEA MBs with theoretical grafting densities of 30%, 50%, and 100% exhibited excellent toxicity profiles in vitro. SFA tests were performed to analyze the lubricative properties of PMSEA MBs. Lubrication performance depends strongly on the grafting density of pendant chains and is tunable. Compared to other polyelectrolyte and zwitterionic hydrophilic MBs, PMSEA MBs exhibited a relatively high coefficient of friction. However, no signs of wear were observed with increasing applied loads, evidencing promising protective properties of PMSEA MBs. Different tribological behaviors were shown for PMSEA MBs with different grafting densities. PMSEA MBs with a grafting density of $\geq$50% exhibited a nonlinear relationship between the coefficient of friction and the applied force. Additionally, highly confined PMSEA MBs exhibited a rheological behavior characteristic for nonentangled polymer melts. Given the straightforward synthesis, excellent toxicity profile, and unique lubricating properties with improved wear protection, we believe that PMSEA MBs are promising candidates for biomedical applications such as biolubricants for medical devices such as contact lenses or for topical applications.

ASSOCIATED CONTENT

Supporting Information

The Supporting Information is available free of charge at https://pubs.acs.org/doi/10.1021/acsapm.2c01468.

Additional experimental details and GPC spectra of PMSEA grafting-from optimization, GPC spectra and structures of all characterized PMSEA samples, and images of cells prior to and after exposure to polymers (PDF)

AUTHOR INFORMATION

Corresponding Authors

Krzysztof Matyjaszewski − *Department of Chemistry, Carnegie Mellon University, Pittsburgh, Pennsylvania 15213, United States;* orcid.org/0000-0003-1960-3402; Email: km3b@andrew.cmu.edu

Xavier Banquy − *Faculty of Pharmacy, Université de Montréal, Montréal, Québec H3C 3J7, Canada; Department of Chemistry, Faculty of Art and Science and Institute of Biomedical Engineering, Faculty of Medicine, Université de Montréal, Montréal, Québec H3C 3J7, Canada;* orcid.org/0000-0002-3342-3179; Email: xavier.banquy@umontreal.ca

Authors

Mateusz Olszewski − *Department of Chemistry, Carnegie Mellon University, Pittsburgh, Pennsylvania 15213, United States*

https://doi.org/10.1021/acsapm.2c01468
ACS Appl. Polym. Mater. 2022, 4, 8564−8573

Duy Anh Pham − *Faculty of Pharmacy, Université de Montréal, Montréal, Québec H3C 3J7, Canada*
Sara González Bolívar − *Faculty of Pharmacy, Université de Montréal, Montréal, Québec H3C 3J7, Canada;* orcid.org/0000-0002-4299-8281
Jean-Michel Rabanel − *Faculty of Pharmacy, Université de Montréal, Montréal, Québec H3C 3J7, Canada;* orcid.org/0000-0001-7552-7606
Michael Martinez − *Department of Chemistry, Carnegie Mellon University, Pittsburgh, Pennsylvania 15213, United States*

Complete contact information is available at: https://pubs.acs.org/10.1021/acsapm.2c01468

Author Contributions

⊥M.O. and D.A.P. contributed equally to this work.

Notes

The authors declare no competing financial interest.

■ ACKNOWLEDGMENTS

Financial support from NSF (DMR 2002747) is acknowledged. X.B. is grateful for the financial support of NSERC (Discovery grant) and the Canada Research Chair program (CRC Tier 2). D.A.P. acknowledges the financial support of the Faculty of Pharmacy at Université de Montréal.

■ REFERENCES

(1) Lee, H.-i.; Pietrasik, J.; Sheiko, S. S.; Matyjaszewski, K. Stimuli-responsive molecular brushes. *Prog. Polym. Sci.* **2010**, *35* (1−2), 24−44.
(2) Sheiko, S. S.; Sumerlin, B. S.; Matyjaszewski, K. Cylindrical molecular brushes: Synthesis, characterization, and properties. *Prog. Polym. Sci.* **2008**, *33* (7), 759−785.
(3) Xie, G.; Martinez, M. R.; Olszewski, M.; Sheiko, S. S.; Matyjaszewski, K. Molecular Bottlebrushes as Novel Materials. *Biomacromolecules* **2019**, *20* (1), 27−54.
(4) Müllner, M. Molecular polymer bottlebrushes in nanomedicine: therapeutic and diagnostic applications. *Chem. Commun.* **2022**, *58* (38), 5683−5716.
(5) Zhao, K.; Gao, Z.; Song, D.; Zhang, P.; Cui, J. Assembly of catechol-modified polymer brushes for drug delivery. *Polym. Chem.* **2022**, *13* (3), 373−378.
(6) Raj, W.; Jerczynski, K.; Rahimi, M.; Przekora, A.; Matyjaszewski, K.; Pietrasik, J. Molecular bottlebrush with pH-responsive cleavable bonds as a unimolecular vehicle for anticancer drug delivery. *Materials Science and Engineering: C* **2021**, *130*, 112439.
(7) Liu, F.; Zhao, X.; Zhang, X.; Zhang, X.; Peng, J.; Yang, H.; Deng, K.; Ma, L.; Chang, C.; Wei, H. Fabrication of theranostic amphiphilic conjugated bottlebrush copolymers with alternating heterografts for cell imaging and anticancer drug delivery. *Polym. Chem.* **2018**, *9* (39), 4866−4874.
(8) Gao, J.; Wen, J.; Hu, D.; Liu, K.; Zhang, Y.; Zhao, X.; Wang, K. Bottlebrush inspired injectable hydrogel for rapid prevention of postoperative and recurrent adhesion. *Bioactive Materials* **2022**, *16*, 27−46.
(9) Vashahi, F.; Martinez, M. R.; Dashtimoghadam, E.; Fahimipour, F.; Keith, A. N.; Bersenev, E. A.; Ivanov, D. A.; Zhulina, E. B.; Popryadukhin, P.; Matyjaszewski, K.; Vatankhah-Varnosfaderani, M.; Sheiko, S. S.Injectable bottlebrush hydrogels with tissue-mimetic mechanical properties. *Sci. Adv.***2022**, *8* (3); DOI: 10.1126/sciadv.abm2469.
(10) Shukla, A.; Singh, A. P.; Maiti, P. Injectable hydrogels of newly designed brush biopolymers as sustained drug-delivery vehicle for melanoma treatment. *Signal Transduct Target Ther* **2021**, *6* (1), 63.
(11) Adibnia, V.; Olszewski, M.; De Crescenzo, G.; Matyjaszewski, K.; Banquy, X. Superlubricity of zwitterionic bottlebrush polymers in the presence of multivalent ions. *J. Am. Chem. Soc.* **2020**, *142* (35), 14843−14847.
(12) Yan, W.; Ramakrishna, S. N.; Spencer, N. D.; Benetti, E. M. Brushes, Graft Copolymers, or Bottlebrushes? The Effect of Polymer Architecture on the Nanotribological Properties of Grafted-from Assemblies. *Langmuir* **2019**, *35* (35), 11255−11264.
(13) Faivre, J.; Shrestha, B. R.; Xie, G.; Delair, T.; David, L.; Matyjaszewski, K.; Banquy, X. Unraveling the Correlations between Conformation, Lubrication, and Chemical Stability of Bottlebrush Polymers at Interfaces. *Biomacromolecules* **2017**, *18* (12), 4002−4010.
(14) Yoshikawa, C.; Sakakibara, K.; Nonsuwan, P.; Yamazaki, T.; Tsujii, Y. Nonbiofouling Coatings Using Bottlebrushes with Concentrated Polymer Brush Architecture. *Biomacromolecules* **2021**, *22* (6), 2505−2514.
(15) Chowdhury, A. U.; Chang, D.; Xu, Y.; Hong, K.; Sumpter, B. G.; Carrillo, J. M. Y.; Doughty, B. Mapping the Interfacial Chemistry and Structure of Partially Fluorinated Bottlebrush Polymers and Their Linear Analogues. *Langmuir* **2021**, *37* (1), 211−218.
(16) Joh, D. Y.; Zimmers, Z.; Avlani, M.; Heggestad, J. T.; Aydin, H. B.; Ganson, N.; Kumar, S.; Fontes, C. M.; Achar, R. K.; Hershfield, M. S.; Hucknall, A. M.; Chilkoti, A. *Architectural Modification of Conformal PEG-Bottlebrush Coatings Minimizes Anti-PEG Antigenicity While Preserving Stealth Properties* **2019**, *8* (8), 1801177.
(17) Hoang Thi, T. T.; Pilkington, E. H.; Nguyen, D. H.; Lee, J. S.; Park, K. D.; Truong, N. P. *Importance of Poly(ethylene glycol) Alternatives for Overcoming PEG Immunogenicity in Drug Delivery and Bioconjugation* **2020**, *12* (2), 298.
(18) Pettersson, T.; Naderi, A.; Makuška, R.; Claesson, P. M. J. L. *Lubrication properties of bottle-brush polyelectrolytes: An AFM study on the effect of side chain and charge density* **2008**, *24* (7), 3336−3347.
(19) Liu, J.; Xu, Y.; Yang, Q.; Li, C.; Hennink, W. E.; Zhuo, R.; Jiang, X. Reduction biodegradable brushed PDMAEMA derivatives synthesized by atom transfer radical polymerization and click chemistry for gene delivery. *Acta Biomaterialia* **2013**, *9* (8), 7758−7766.
(20) Dalal, R. J.; Kumar, R.; Ohnsorg, M.; Brown, M.; Reineke, T. M. Cationic Bottlebrush Polymers Outperform Linear Polycation Analogues for pDNA Delivery and Gene Expression. *ACS Macro Lett.* **2021**, *10*, 886−893.
(21) Banquy, X.; Burdynska, J.; Lee, D. W.; Matyjaszewski, K.; Israelachvili, J. Bioinspired Bottle-Brush Polymer Exhibits Low Friction and Amontons-like Behavior. *J. Am. Chem. Soc.* **2014**, *136* (17), 6199−6202.
(22) Faivre, J.; Shrestha, B. R.; Burdynska, J.; Xie, G.; Moldovan, F.; Delair, T.; Benayoun, S.; David, L.; Matyjaszewski, K.; Banquy, X. Wear Protection without Surface Modification Using a Synergistic Mixture of Molecular Brushes and Linear Polymers. *ACS Nano* **2017**, *11* (2), 1762−1769.
(23) Xia, Y.; Adibnia, V.; Shan, C.; Huang, R.; Qi, W.; He, Z.; Xie, G.; Olszewski, M.; De Crescenzo, G.; Matyjaszewski, K.; Banquy, X.; Su, R. Synergy between Zwitterionic Polymers and Hyaluronic Acid Enhances Antifouling Performance. *Langmuir* **2019**, *35* (48), 15535−15542.
(24) Xia, Y.; Adibnia, V.; Huang, R.; Murschel, F.; Faivre, J.; Xie, G.; Olszewski, M.; De Crescenzo, G.; Qi, W.; He, Z.; Su, R.; Matyjaszewski, K.; Banquy, X. Biomimetic Bottlebrush Polymer Coatings for Fabrication of Ultralow Fouling Surfaces. *Angewandte Chemie - International Edition* **2019**, *58* (5), 1308−1314.
(25) Oh, K.-I.; Baiz, C. R. Crowding Stabilizes DMSO−Water Hydrogen-Bonding Interactions. *J. Phys. Chem. B* **2018**, *122* (22), 5984−5990.
(26) Xu, X.; Huang, X.; Chang, Y.; Yu, Y.; Zhao, J.; Isahak, N.; Teng, J.; Qiao, R.; Peng, H.; Zhao, C.-X.; Davis, T. P.; Fu, C.; Whittaker, A. K. Antifouling Surfaces Enabled by Surface Grafting of Highly Hydrophilic Sulfoxide Polymer Brushes. *Biomacromolecules* **2021**, *22* (2), 330−339.
(27) Mackenzie, M. C.; Shrivats, A. R.; Konkolewicz, D.; Averick, S. E.; McDermott, M. C.; Hollinger, J. O.; Matyjaszewski, K. Synthesis of Poly(meth)acrylates with Thioether and Tertiary Sulfonium

Groups by ARGET ATRP and Their Use as siRNA Delivery Agents. *Biomacromolecules* **2015**, *16* (1), 236−245.
(28) Işık, D.; Joshi, A. A.; Guo, X.; Rancan, F.; Klossek, A.; Vogt, A.; Rühl, E.; Hedtrich, S.; Klinger, D. Sulfoxide-functionalized nanogels inspired by the skin penetration properties of DMSO. *Biomaterials Science* **2021**, *9* (3), 712−725.
(29) Hofmann, V.; Ringsdorf, H.; Muacevic, G. Pharmakologisch aktive polymere, 8.Poly[2-(methylsulfinyl)äthylacrylat]e und ihre vermittelnde wirkung auf die transkutane resorption von pharmaka. *Makromol. Chem.* **1975**, *176* (7), 1929−1943.
(30) Garnier, S.; Laschewsky, A. Synthesis of New Amphiphilic Diblock Copolymers and Their Self-Assembly in Aqueous Solution. *Macromolecules* **2005**, *38* (18), 7580−7592.
(31) Li, S.; Chung, H. S.; Simakova, A.; Wang, Z.; Park, S.; Fu, L.; Cohen-Karni, D.; Averick, S.; Matyjaszewski, K. Biocompatible Polymeric Analogues of DMSO Prepared by Atom Transfer Radical Polymerization. *Biomacromolecules* **2017**, *18* (2), 475−482.
(32) Yu, Y.; Xu, W.; Huang, X.; Xu, X.; Qiao, R.; Li, Y.; Han, F.; Peng, H.; Davis, T. P.; Fu, C.; Whittaker, A. K. Proteins Conjugated with Sulfoxide-Containing Polymers Show Reduced Macrophage Cellular Uptake and Improved Pharmacokinetics. *ACS Macro Lett.* **2020**, *9* (6), 799−805.
(33) Işık, D.; Quaas, E.; Klinger, D. Thermo- and oxidation-sensitive poly(meth)acrylates based on alkyl sulfoxides: dual-responsive homopolymers from one functional group. *Polym. Chem.* **2020**, *11* (48), 7662−7676.
(34) Israelachvili, J. Thin film studies using multiple-beam interferometry. *Journal of Colloid & Interface Science* **1973**, *44* (2), 259−272.
(35) Israelachvili, J.; Min, Y.; Akbulut, M.; Alig, A.; Carver, G.; Greene, W.; Kristiansen, K.; Meyer, E.; Pesika, N.; Rosenberg, K.; et al. Recent advances in the surface forces apparatus (SFA) technique. *Rep. Prog. Phys.* **2010**, *73* (3), 036601.
(36) Martinez, M. R.; Sobieski, J.; Lorandi, F.; Fantin, M.; Dadashi-Silab, S.; Xie, G.; Olszewski, M.; Pan, X.; Ribelli, T. G.; Matyjaszewski, K. Understanding the Relationship between Catalytic Activity and Termination in photoATRP: Synthesis of Linear and Bottlebrush Polyacrylates. *Macromolecules* **2020**, *53* (1), 59−67.
(37) Ribelli, T. G.; Konkolewicz, D.; Bernhard, S.; Matyjaszewski, K. How are Radicals (Re)Generated in Photochemical ATRP? *J. Am. Chem. Soc.* **2014**, *136* (38), 13303−13312.
(38) Erdemir, A.; Erck, R. A.; Robles, J. Relationship of hertzian contact pressure to friction behavior of self-lubricating boric acid films. *J. Surface coatings Technology* **1991**, *49* (1−3), 435−438.
(39) Drummond, C.; Marinov, G.; Richetti, P. J. L. Reinforcement of a Surfactant Boundary Lubricant Film by a Hydrophilic− Hydrophilic Diblock Copolymer. *Langmuir* **2008**, *24* (4), 1560−1565.
(40) Luengo, G.; Israelachvili, J.; Granick, S. Generalized effects in confined fluids: new friction map for boundary lubrication. *Wear* **1996**, *200* (1−2), 328−335.
(41) Nomura, A.; Ohno, K.; Fukuda, T.; Sato, T.; Tsujii, Y. Lubrication mechanism of concentrated polymer brushes in solvents: effect of solvent viscosity. *Polym. Chem.* **2012**, *3* (1), 148−153.
(42) Subbotin, A.; Semenov, A.; Manias, E.; Hadziioannou, G.; Ten Brinke, G. Nonlinear rheology of polymer melts under shear flow. *Macromolecules* **1995**, *28* (11), 3898−3900.
(43) Luengo, G.; Schmitt, F.-J.; Hill, R.; Israelachvili, J. Thin film rheology and tribology of confined polymer melts: contrasts with bulk properties. *Macromolecules* **1997**, *30* (8), 2482−2494.
(44) Raviv, U.; Frey, J.; Sak, R.; Laurat, P.; Tadmor, R.; Klein, J. Properties and interactions of physigrafted end-functionalized poly (ethylene glycol) layers. *Langmuir* **2002**, *18* (20), 7482−7495.
(45) Daniel, W. F.; Burdyńska, J.; Vatankhah-Varnoosfaderani, M.; Matyjaszewski, K.; Paturej, J.; Rubinstein, M.; Dobrynin, A. V.; Sheiko, S. S. Solvent-free, supersoft and superelastic bottlebrush melts and networks. *Nature materials* **2016**, *15* (2), 183−189.

https://doi.org/10.1021/acsapm.2c01468
ACS Appl. Polym. Mater. 2022, 4, 8564−8573